Workshop on Material Appearance Modeling (2017)
H. Rushmeier and R. Klein (Editors)

Experimental Analysis of BSDF Models

Murat Kurt[1]

[1]International Computer Institute, Ege University

Abstract

The Bidirectional Scattering Distribution Function (BSDF) describes the appearance of an optically thin, translucent material by its interaction with light at a surface point. Various BSDF models have been proposed to represent BSDFs. In this paper, we experimentally analyze a few of BSDF models in terms of their accuracy to represent measured BSDFs, their required storage sizes and computation times. To make a fair comparison of BSDF models, we measured three samples of optically thin, translucent materials (hunter douglas, orange glass, structured glass) by using pgII gonio-photometer. Based on rendered images, required storage sizes and computation times, we compare the performance of the BSDF models. We show that data-driven BSDF models give a more accurate representation of measured BSDFs, while data-driven BSDF models require much more storage sizes and computation times. We also show that BSDF measurements from highly anisotropic translucent materials can not be expressed by an analytical BSDF model visually correctly.

Categories and Subject Descriptors (according to ACM CCS): I.3.7 [Computer Graphics]: Three-Dimensional Graphics and Realism—Color, shading, shadowing, and texture

1. Introduction

Photo-realistic rendering can be seen as a variant of computer graphics that addresses light interaction and accurate descriptions of materials involved in a scene. Optically thin, translucent materials, such as papers, glasses and daylight redirecting films, are represented by Bidirectional Scattering Distribution Functions (BSDFs) [NRH*77]. The BSDF is a sum of Bidirectional Reflectance Distribution Function (BRDF) and Bidirectional Transmittance Distribution Function (BTDF) [NRH*77], therefore it represents both light reflection and light transmission of translucent materials.

In photo-realistic rendering process, measured BSDF data can be represented by an analytical BSDF model [WMLT07] or a data-driven BSDF model [WKB12, KWB16]. Since measuring four-dimensional (4D) BSDF data is a very time consuming process, there is only the Building Material Examples (BME) BSDF database [AB14] in the literature. The BME database was constructed by Apian-Bennewitz [AB14], and it includes BRDF, BTDF and BSDF measurements. The BME database includes measurements from frequently used materials, and it does not include measurements from highly anisotropic or complex translucent materials, such as structured glasses [AB14]. We feel that there is a need for a large BSDF database, which consists of measurements from isotropic, anisotropic and complex translucent materials. Although an extensive comparison and evaluation of BRDF models was presented by Ngan et al. [NDM05], we feel that an experimental analysis and comparison of BSDF models are needed.

In this paper, we experimentally analyze performance of BSDF models by comparing their abilities to represent real measured BSDF data. To make a fair comparison on real measured BSDF data, we captured BSDF data from three translucent materials (hunter douglas, orange glass, structured glass), which consist of isotropic (orange glass) to highly anisotropic (structured glass) translucent materials. In this work, we also use isotropic BSDF measurements from the BME database [AB14]. Our study can be seen as a guide to practitioners in engineering and other fields for capturing BSDF data from optically thin, translucent materials and choosing right BSDF model that meets their needs. Our BSDF measurements can also be seen as a starting point for constructing a large BSDF database.

2. BSDF Data Set and Acquisition

In this work, we measure optically thin translucent materials by using pgII gonio-photometer [AB14]. A general overview of pgII gonio-photometer can be seen in Figure 1. pgII gonio-photometer consists of a sample holder, a light source and a detector. A variety of sample holders can be used depending on the material. Light sources are mounted on a standard optical bench, including collimating optics and custom baffles. The detector is mounted at the end of a linkage consisting of two light weight arms, and it's moved fast at a constant distance around the sample center. pgII gonio-photometer measures BSDF data in spherical coordinate system $(\theta_i, \phi_i, \theta_o, \phi_o)$. Measured BSDF data isn't regularly sampled at both incoming (θ_i, ϕ_i) and outgoing (θ_o, ϕ_o) directions. While pgII

DOI: 10.2312/mam.20171330

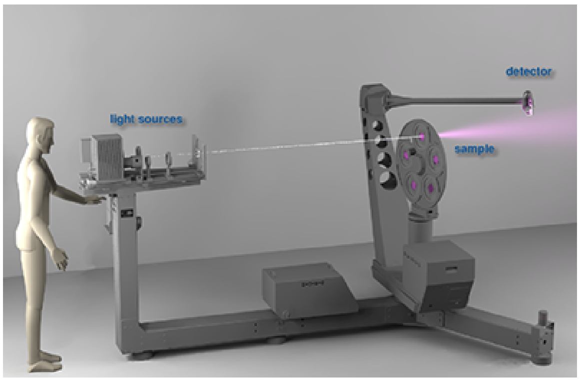

Figure 1: *An overview of pgII gonio-photometer [AB14] (image from [AB14]).*

gonio-photometer allows many outgoing angle measurements, it allows only a few number of incoming angle measurements. Therefore, we get BSDF measurements that are irregular and sparse. While these BSDF measurements can be represented by an analytical BSDF model, they must be preprocessed before representing and rendering by a data-driven BSDF representation.

By using pgII gonio-photometer, we measured BSDF data from three samples of optically thin, translucent materials, namely hunter douglas, orange glass, and structured glass. Our real measurement setup can be seen in Figure 2. Photographs of measured translucent materials can be seen in Figure 3(first column). Structure of hunter douglas is mostly reflective and diffuse. Orange glass material is isotropic and glossy. Structured glass is anisotropic and glossy. We constructed a BSDF database, which includes measurements from all of these measured translucent materials. Our BSDF database can be used for validation, simulation and comparison purposes. The acquisition time amounted to approximately two days for each BSDF measurement.

3. BSDF Models

We choose one analytical BSDF model and one data-driven BSDF model for our analysis: Walter et al.'s [WMLT07] analytical BSDF model, and Ward et al.'s [WKB12] data-driven BSDF representation. These BSDF models differ in their degrees of freedom and goals, and we focus on the numerical ability to fit our measured BSDF data, computation times and storage needs.

Walter et al.'s [WMLT07] analytical model is based on the microfacet theory and it's for representing rough glass material. In their work, Walter et al. introduced GGX microfacet normal distribution which works extremely well when it's compared to Beckmann distribution for representing rough translucent materials. Walter et al. also proposed importance sampling techniques for their BSDF model, which is essential to Monte Carlo rendering algorithms. The reflection part of Walter et al. BSDF model is similar to Cook-Torrance BRDF model [CT81], and we restrict reflection part to have only one specular lobe and the diffuse contribution to be Lambertian. Walter et al.'s BSDF model can be formalized as:

$$
\begin{aligned}
f(\omega_i,\omega_o) &= \frac{k_d}{\pi} \\
&+ k_{sr}\frac{F(\omega_i,\omega_{hr},f_{0r})G(\omega_i,\omega_o,\omega_{hr},\alpha_r)D(\omega_{hr},\alpha_r)}{4|\omega_i\cdot\omega_n||\omega_o\cdot\omega_n|} \\
&+ k_{st}\frac{|\omega_i\cdot\omega_{ht}||\omega_o\cdot\omega_{ht}|}{|\omega_i\cdot\omega_n||\omega_o\cdot\omega_n|} \\
&\times \frac{\eta_o^2(1-F(\omega_i,\omega_{ht},f_{0t}))G(\omega_i,\omega_o,\omega_{ht},\alpha_t)D(\omega_{ht},\alpha_t)}{(\eta_i(\omega_i\cdot\omega_{ht})+\eta_o(\omega_o\cdot\omega_{ht}))^2}, \qquad (1)
\end{aligned}
$$

where ω_i is incoming light vector, ω_o is outgoing view vector, ω_n is surface normal vector, $\omega_{hr} = (\omega_i+\omega_o)/\parallel \omega_i+\omega_o \parallel$ is halfway reflection vector, $\omega_{ht} = -(\eta_i\omega_i+\eta_o\omega_o)/\parallel \eta_i\omega_i+\eta_o\omega_o \parallel$ is halfway transmission vector, $F(\cdot)$ is Fresnel term [CT81], $G(\cdot)$ is shadowing-masking term, $D(\cdot)$ is microfacet normal distribution function, k_d is diffuse coefficient, k_{sr} is specular reflection coefficient, k_{st} is specular transmission coefficient, η_i is index of refraction for the incident side of the surface, η_o is index of refraction for the transmitted side of the surface, α_r is width parameter for the incident side of the surface, α_t is width parameter for the transmitted side of the surface, f_{0r} is Fresnel coefficient for the incident side of the surface, and f_{0t} is Fresnel coefficient for the transmitted side of the surface. To compute Fresnel term, we use Schlick approximation [Sch94] as $F(\omega_i,\omega_h,f_0) = f_0+(1-f_0)(1-(\omega_i\cdot\omega_h))^5$. To compute $G(\cdot)$ term, we use Smith approximation as $G(\omega_i,\omega_o,\omega_h,\alpha) \approx G_1(\omega_i,\omega_h,\alpha)G_1(\omega_o,\omega_h,\alpha)$. To compute $G_1(\cdot)$ and $D(\cdot)$, we use the following GGX distribution:

$$D(\omega_h,\alpha) = \frac{\alpha^2\chi^+(\omega_h\cdot\omega_n)}{\pi\cos^4\theta_h(\alpha^2+\tan^2\theta_h)^2}, \qquad (2)$$

$$G_1(\omega,\omega_h,\alpha) = \chi^+\left(\frac{\omega\cdot\omega_h}{\omega\cdot\omega_n}\right)\frac{2}{1+\sqrt{1+\alpha^2\tan^2\theta}}, \qquad (3)$$

where $\chi^+(a)$ is the positive function, which equals to one if $a>0$ and zero if $a\leq 0$. One of the core parts of our analysis is to fit measured BSDF data to Walter et al.'s analytical model. In this work, we extend Ngan et al.'s [NDM05] fitting procedure to represent measured BSDFs by Walter et al.'s analytical BSDF model. We apply a constrained nonlinear optimization technique, and we estimate $\alpha_r,\alpha_t,\eta_o,\eta_i,f_{0r},f_{0t}$ terms nonlinearly by using a constrained minimization algorithm. k_d,k_{sr},k_{st} terms are computed analytically as a subprocedure based on a linear least square optimization. To optimize fitting results for finding a global minimum, we restart the optimization with a different set of initial guesses and we take a set of parameters which leads the minimum L^2 error.

Ward et al.'s [WKB12] data-driven BSDF framework includes two data-driven BSDF representations: Matrix-based BSDF representation and Tensor tree BSDF representation. This framework is readily available in RADIANCE renderer [LS98] as an XML representation and an Open Source C library. The library allows for the efficient representation, query and Monte Carlo importance sampling of real-world BSDFs in a model-free framework. In this work, we select to use Tensor tree BSDF representation, because it helps to represent highly peaked data more accurately by subdividing BSDF data adaptively in different regions of the distribution. Tensor tree BSDF representation helps to keep closely associated BSDF values near each other for a convenient subdivision. Tensors

Figure 2: *Real photographs from our pgII gonio-photometer setup.*

can be considered as a direct extension of vectors and matrices. We use rank-3 tensors and rank-4 tensors to represent isotropic and anisotropic BSDF data, respectively. While isotropic BSDF data is represented in $(\theta_i, \theta_o, \phi_{diff} = \phi_o - \phi_i)$ parameters, anisotropic BSDF data is represented in $(\theta_i, \phi_i, \theta_o, \phi_o)$ parameters. In Tensor tree BSDF representation, to map dimensions in Tensor tree BSDF representation to dimensions on each hemisphere, Shirley and Chiu mapping [SC97] is used. Since our BSDF measurements are sparse and irregular, we need to fill these BSDF measurements accurately to be able to represent them with Tensor tree BSDF representation. In this work, we use Ward et al.'s [WKB14] Lagrangian based interpolation technique for filling our sparse set of incident angle measurements. Ward et al.'s [WKB14] method for reconstructing a complete BSDF from sparse, irregular measurements proceeds in three stages. For each incident direction, measured BSDF values are fitted by a sum of Gaussian lobes. Then, a spherical Delaunay triangulation of the incident directions are constructed. Finally, for each edge of the triangulation, a transport plan is computed for shifting Gaussian lobes in the first vertex to Gaussian lobes in the second vertex. To make an interpolation inside the triangles of a spherically Delaunay triangulated mesh, a method similar to a nested linear interpolation of the transport plan is used. The other details of Tensor tree representation and Langrangian based interpolation technique can be found in [WKB12] and [WKB14], respectively.

4. Experimental Results

To investigate abilities of BSDF models, we used our BSDF measurements and BSDF measurements from BME database [AB14]. The nonlinear parameters of Walter et al. [WMLT07] BSDF model is estimated by using `fmincon` [WMNO11] function in MATLAB library. `fmincon` provides a constrained nonlinear optimization, which attempts to find a minimum of a function of several variables starting at an initial estimate. We optimize L^2 errors [NDM05] in this fitting procedure, and linear parameters are estimated as a subprocedure based on a linear least square optimization. To represent BSDF measurements with Ward et al. [WKB12] Tensor tree BSDF representation, we first interpolated it by Ward et al. [WKB14] interpolation technique. To simulate both Walter et al.'s BSDF model and Ward et al.'s interpolation technique in RADIANCE [LS98], tensor tree BSDF representations are constructed by using `bsdf2ttree` function in RADIANCE. Figure 3 and Figure 4 shows visual comparison of both BSDF representations. While Figure 3 includes comparisons based on our BSDF measurements, Figure 4 includes comparisons based on isotropic BSDF measurements from BME database [AB14]. Since Walter et al. BSDF model only considers single scattering term, and it does not handle multiple scattering terms inside the material volumes, there are some inaccuracies and color decays in the representations of materials. Ward et al.'s BSDF representation has ability to handle more complex materials visually plausibly, and it try to represent both single scattering and multiple scattering inside the material volumes.

Furthermore, we compared storage requirements and computation times of the investigated BSDF representations. Table 1 reports storage requirements that are used to render images in Figure 3. Although, Ward et al.'s data-driven BSDF representation provides $10\times$ compression, Walter et al.'s analytical BSDF model guarantees the most compact representation. On a 4-core laptop, average computation times of Walter et al.'s BSDF model and Ward et al.'s BSDF interpolation technique are 12 minutes, and 46 minutes, respectively.

5. Conclusion

In this paper, we measured BSDF data from 3 different optically thin, translucent materials, and made experimental analysis on these BSDF measurements and BSDF measurements from BME database by representing them with various BSDF models. We have shown that compared to Walter et al.'s BSDF model, Ward et al.'s data-driven BSDF representation provides more accurate representations, while it requires $\sim 60\times$ storage needs and $\sim 4\times$ computation times.

We're planing to make publicly available our BSDF measurements and fitting results for giving a start to construct a huge BSDF database.

Acknowledgements

This work was supported by the Scientific and Technical Research Council of Turkey (Project No: 115E203), the Scientific Research Projects Directorate of Ege University (Project No:2015/BİL/043). Author would like to thank all collaborators that have helped when preparing this work.

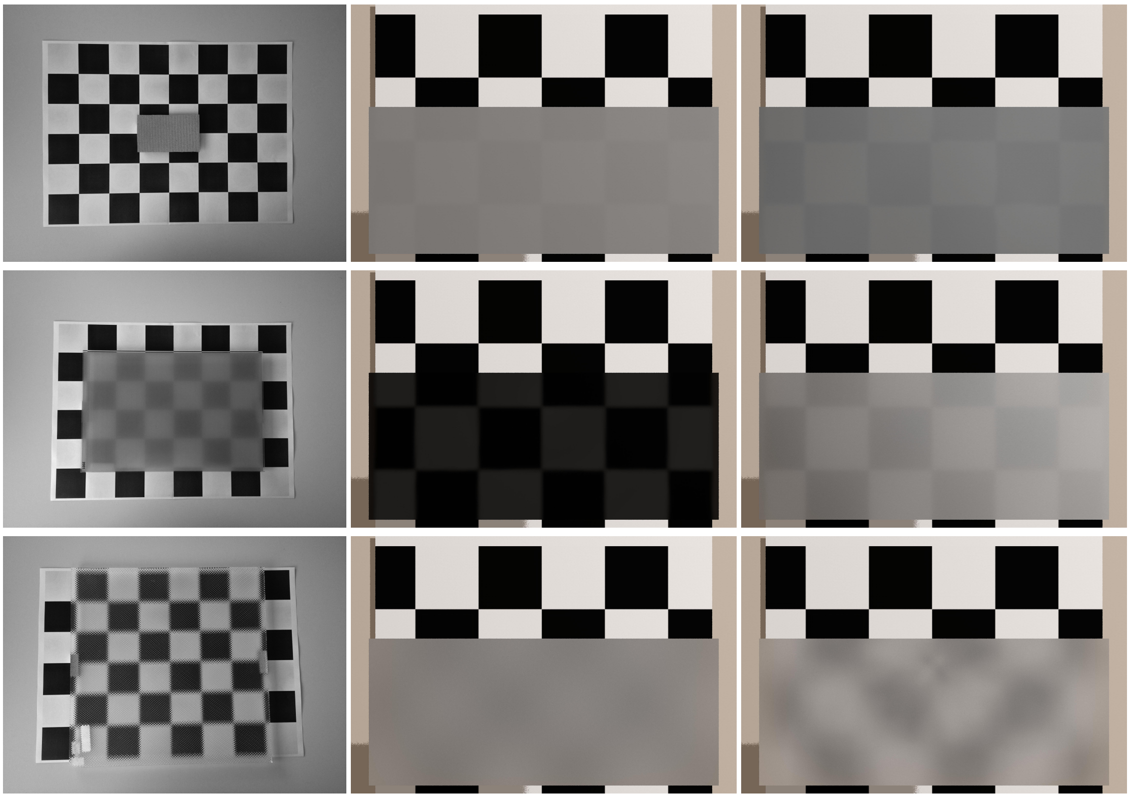

Figure 3: *We qualitatively compare Walter et al.'s analytical BSDF model [WMLT07] with Ward et al.'s data-driven BSDF model [WKB12] using three measured BSDFs and photographs. First, second and third rows are hunter douglas, orange glass and structured glass materials, respectively. First, second and third columns are real photographs, Walter et al.'s BSDF model [WMLT07], and Ward et al.'s BSDF model [WKB12], respectively.*

Material Name	Measured	Walter et al. [WMLT07]	Ward et al. [WKB12]
Hunter douglas	257MB	0.25MB	23.7MB
Orange glass	158MB	0.28MB	18.6MB
Structured glass	195.8MB	0.76MB	20.6MB

Table 1: *Required storage spaces of BSDF measurements and BSDF representations for various materials.*

References

[AB14] Apian-Bennewitz P.: Building material examples (BME) BRDF and BSDF database., 2014. URL: http://www.pab.eu/gonio-photometer/demodata/bme/. 1, 2, 3, 5

[CT81] Cook R. L., Torrance K. E.: A reflectance model for computer graphics. *Computer Graphics 15*, 3 (1981), 307–316. (Proc. SIGGRAPH '81). 2

[KWB16] Kurt M., Ward G., Bonneel N.: A data-driven bsdf framework. In *ACM SIGGRAPH 2016 Posters* (Anaheim, California, 2016), SIGGRAPH '16, ACM, pp. 31:1–31:2. URL: http://doi.acm.org/10.1145/2945078.2945109, doi:10.1145/2945078.2945109. 1

[LS98] Larson G. W., Shakespeare R.: *Rendering with Radiance: the art and science of lighting visualization*. Morgan Kaufmann Publishers Inc., 1998. 2, 3

[NDM05] Ngan A., Durand F., Matusik W.: Experimental analysis of BRDF models. In *Proc. of Eurographics Symposium on Rendering* (2005), pp. 117–126. 1, 2, 3

[NRH*77] Nicodemus F. E., Richmond J. C., Hsia J. J., Ginsberg I. W., Limperis T.: *Geometrical Considerations and Nomenclature for Reflectance*. Monograph, National Bureau of Standards (US), Oct. 1977. 1

[SC97] Shirley P., Chiu K.: A low distortion map between disk and square. *Journal Graphics Tools 2*, 3 (1997), 45–52. 3

[Sch94] Schlick C.: An inexpensive BRDF model for physically-based rendering. *Computer Graphics Forum 13*, 3 (1994), 233–246. (Proc. Eurographics '94). 2

[WKB12] Ward G., Kurt M., Bonneel N.: *A Practical Framework for Sharing and Rendering Real-World Bidirectional Scattering Distribution Functions*. Tech. Rep. LBNL-5954E, Lawrence Berkeley National Laboratory, October 2012. 1, 2, 3, 4, 5

[WKB14] Ward G., Kurt M., Bonneel N.: Reducing anisotropic bsdf measurement to common practice. In *Proceedings of the*

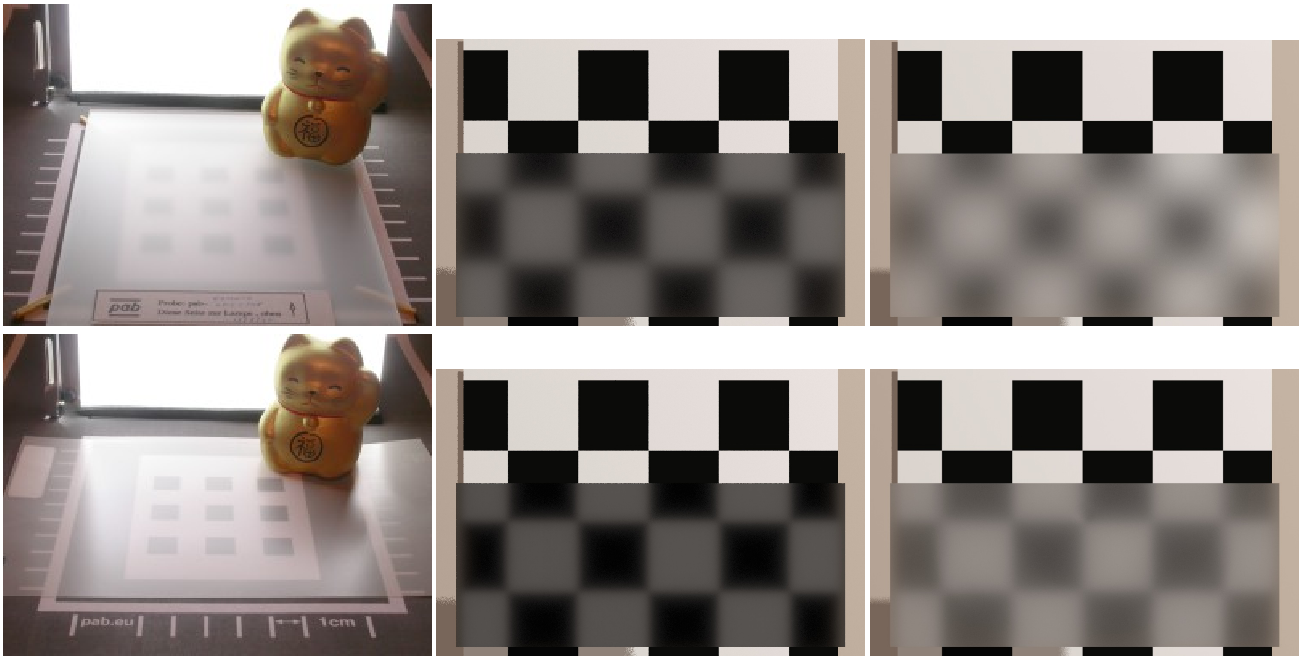

(a) Photograph (b) Walter et al. [WMLT07] (c) Ward et al. [WKB12]

Figure 4: *Ward et al. [WKB12] BSDF representation (c) captures the appearance of isotropic translucent materials more accurately, when it's compared to Walter et al. [WMLT07] BSDF model (b).* $L02-148$ *(first row) and* vk_op10 *(second row) (a) are from the BME database [AB14].*

2nd Eurographics Workshop on Material Appearance Modeling: Issues and Acquisition (Lyon, France, 2014), Klein R., Rushmeier H., (Eds.), MAM '14, Eurographics Association, pp. 5–8. URL: http://diglib.eg.org/EG/DL/WS/MAM/MAM2014/005-008.pdf, doi:10.2312/mam.20141292. 3

[WMLT07] Walter B., Marschner S. R., Li H., Torrance K. E.: Microfacet models for refraction through rough surfaces. In *Proceedings of the 18th Eurographics Conference on Rendering Techniques* (2007), EGSR'07, pp. 195–206. 1, 2, 3, 4, 5

[WMNO11] Waltz R., Morales J., Nocedal J., Orban D.: An interior algorithm for nonlinear optimization that combines line search and trust region steps. *Mathematical Programming 107*, 3 (2011), 391–408. 3